Spectrum of infantile esotropia in primates: Behavior, brains, and orbits

Lawrence Tychsen, MD,[a,b] Michael Richards,[c] Agnes Wong, MD, PhD,[a,c] Paul Foeller, MS,[a] Andreas Burhkalter, PhD,[b] Anita Narasimhan, MS,[d] and Joseph Demer, MD, PhD[d]

INTRODUCTION Recent studies of human infants have described a spectrum of early-onset esotropia, from small angle to large heterotropias. We report here a similar spectrum of early-onset esotropia in infant monkeys, with emphasis on the relationship between visuomotor deficits, central nervous system circuitry, and orbital anatomy.

METHODS Eye movements were recorded in macaque monkeys with natural, infantile-onset esotropia (n = 7) and in control monkeys (n = 2) to assess alignment, latent nystagmus, dissociated vertical deviation (DVD), and pursuit/optokinetic nystagmus (OKN) asymmetries. Acuity was measured by preferential-looking technique or spatial sweep visual-evoked potentials. Geniculo-striate pathways were then analyzed with neuroanatomic tracers and ocular dominance column labels. Extraocular muscles were examined by high-resolution magnetic resonance imaging (MRI) and anatomic sectioning of whole orbits.

RESULTS Esotropia ranged from 4 to 13.5° (7–24$^{\Delta}$) with fixation preference (if any) varying idiosyncratically (as in human). Severity of ocular motor dysfunction (ie, nystagmus velocity, DVD amplitude, pursuit-OKN nasal bias index) increased as the magnitude of esotropia angle. Animals with greater ocular motor deficits tended to have greater visual area V1 (striate cortex) neuroanatomic deficits, evident as fewer binocular horizontal connections in V1. Orbital MRI/anatomic analysis showed no difference in horizontal rectus cross-sectional areas, muscle paths, innervation densities, or cytoarchitecture compared with normal animals.

CONCLUSIONS The infantile esotropia spectrum in nonhuman primates is remarkably similar to that reported in human infants. Concomitant esotropia in these primates cannot be ascribed to abnormalities of the extraocular muscles or orbit. These findings, combined with epidemiologic studies of humans, suggest that perturbations of cerebral binocular pathways in early development are the primary cause of the infantile esotropia syndrome. (J AAPOS 2008;12:375–380)

Recent studies have revealed that infantile esotropia can be produced reliably in infant primates if they experience binocular decorrelation in the first weeks of visuomotor development.[2,3] The magnitude of the oculomotor deficits in these primates is related systematically to the duration of binocular decorrelation. These studies have also revealed a general concordance between the severity of the behavioral deficits and the reduction of binocular anatomic connections in the primary visual cortex.[23]

The purpose of this study was to determine if primates with naturally occurring infantile esotropia show a similar functional-structural concordance. Subsumed under this general aim were two subordinate questions. First, is infantile esotropia an all-or-none phenomenon, or do primates display a range of abnormality—some mild, some severe? Second, is the primary mechanism a maldevelopment of cerebral visuomotor circuits or alternatively an abnormality of the horizontal rectus muscles of the orbit?

See accompanying editorial on p. 324.

Author affiliations: [a]Department of Ophthalmology and Visual Sciences, Washington University School of Medicine, St. Louis, Missouri; [b]Department of Anatomy and Neurobiology, Washington University School of Medicine, St. Louis, Missouri; [c]Department of Ophthalmology and Vision Sciences, University of Toronto, Toronto, Ontario, Canada; and [d]Department of Ophthalmology, and Neuroscience and Neurology Department, University of California, Los Angeles, California

Presented at the 33rd Annual Meeting of the American Association for Pediatric Ophthalmology and Strabismus, Seattle, Washington, April 2007.

This work was supported by NIH grant EY10214.

Submitted April 11, 2007.

Revision accepted November 5, 2007.

Published online March 4, 2008.

Reprint requests: Lawrence Tychsen, MD, St. Louis Children's Hospital at Washington University Medical Center, One Children's Place, Suite 2S-89, St. Louis, MO 63110 (email: tychsen@vision.wustl.edu)

1091-8531/2008/$35.00 + 0

doi:10.1016/j.jaapos.2007.11.010

Animals and Methods

Eye movements were recorded in seven naturally strabismic, adult macaque monkeys who had spontaneous onset of esotropia in the first 2 months of life and in two control monkeys. The strabismic animals ranged in age from 3 to 19 years (mean weight, 5.4 kg), and the controls ranged in age from 3 to 6 years (mean weight, 5.4 kg). Eye movements were recorded using a digital video (modified Hirshberg[4]) technique (n = 4) and/or

binocular magnetic search coil method[5] (n = 5). Recordings were obtained under conditions of monocular and binocular viewing, using a mechanical, opaque metal occluder positioned before either eye or an opaque soft occluder lens. In animals implanted with binocular search coils, automated cover testing was performed using liquid crystal shutter goggles.[5,6] To determine the presence or absence of amblyopia, fixation preferences were observed and grating acuities were obtained using a preferential looking technique (n = 4) or spatial sweep visual-evoked potentials (n = 5). Cycloplegic refractions and funduscopic examinations were also performed in each animal. Eye alignment was assessed for concomitance at cardinal positions of gaze (±20° horizontally and vertically). Fixation, pursuit, and/or optokinetic nystagmus (OKN) was recorded while the animal viewed stationary or moving spots of light and large-field OKN stripes.

After completion of behavioral studies, anatomic analysis of the orbits (n = 4)[7-9] and horizontal connections between ocular dominance columns (ODC) of the visual cortex (n = 8)[10,11] was carried out using standard methods described in previous studies. Briefly, high-resolution magnetic resonance imaging (MRI) images were obtained of each orbit, followed by analysis of coronal serial sections (10 μm thickness) stained using Masson's trichrome (muscle and connective tissue) and van Gieson's (elastin fibers) methods. The visual cortex (area V1) was analyzed for binocular horizontal connections between ODCs of opposite ocularity in each cerebral hemisphere. The ocularity of ODCs was determined by transneuronal labeling using wheat germ agglutinin-horseradish peroxidase or tritiated proline injected into the vitreous cavity of one eye. Horizontal connections within V1 were labeled by injection of a second label, biotinylated dextran amine (BDA), into multiple ODCs. Injections of the labels were performed under general anesthesia approximately 7 to 10 days before terminal anesthesia, brain perfusion, and histologic processing. All experiments were performed in compliance with the Association for Research in Vision and Ophthalmology resolution on the use of animals in research and were approved by Washington University Animal Care and Use Committee.

Results

Ocular Motor Deficits

The strabismic monkeys had onset of their esodeviations in the first 2 months of life. Four (57%) of the 7 (monkeys T, Z, A, and H) alternated fixation and had normal grating visual acuities in each eye. The other 3 (43%) also had equivalent grating acuities in the two eyes but showed small fixation preferences; 2 of these monkeys had a right-eye preference (K and L) and 1 had a left-eye preference (monkey J). Cycloplegic refractive errors in the seven strabismic and two normal monkeys were mild to moderately hyperopic (range, +0.5 to +5.5 D; esotropic mean refractive error +2.37 D, control +2.85). Spherical equivalent refractive error did not correlate with magnitude of esodeviation (r = 0.02, p = 0.96) when fixating targets at the standard viewing distance employed (1 m). However, the 3 strabismic animals with the largest hyperopic refractive errors (K, J, and L) did show increased deviations when fixating near (33 cm viewing distance) targets (mean near vs distance increase + 5.3°). They could, therefore, be classified as mixed mechanism, infantile, and refractive accommodative esotropia.

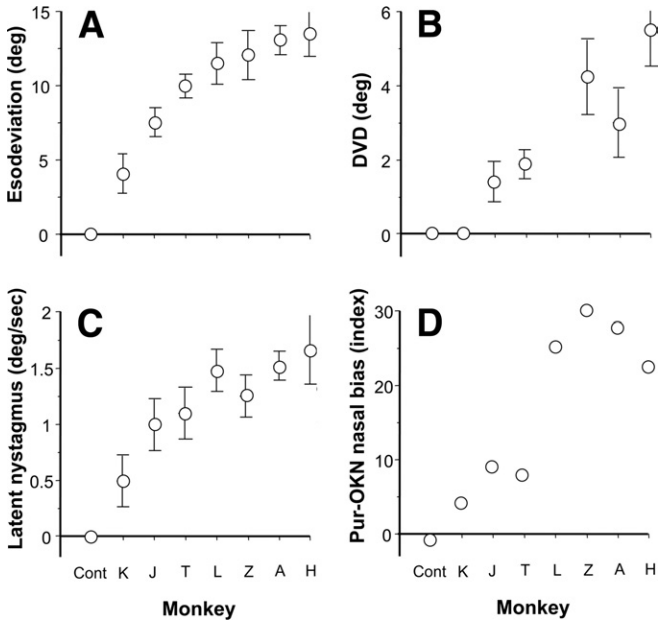

FIG 1. Ocular motor signs in the strabismic monkeys. Animals are ordered along the *x*-axis according to magnitude of esotropia. (A) Esodeviation measured under conditions of binocular viewing of a target in primary position at 1 m viewing distance (mean ± SD). (B) Magnitude of dissociated vertical deviation. Averages pooled from dissociated vertical deviation (DVD) in both eyes if bilateral and from one eye if unilateral. (C) Velocity of latent nystagmus under conditions of monocular viewing (one eye covered). Averages pooled from velocities recorded when viewing with the right and then the left eye. (D) Smooth pursuit or optokinetic nystagmus (OKN) nasalward bias index (NBI, see text). Average NBI for viewing moving target with the right, then the left, eye.

Figure 1A plots the mean esodeviation (constant heterotropia) in primary position for each strabismic monkey, ordered from smallest to largest. Testing at cardinal gaze positions showed that the deviations were concomitant to within ±2.5° (4.4$^{\Delta}$). Two monkeys (H and T) had small A-pattern deviations (slightly greater eso in upgaze and slightly less eso in downgaze). Figure 1B shows the results of cover testing conducted to detect the presence of a dissociated vertical deviation (DVD) in 6 of the 7 esotropic monkeys. Of the 6, 5 had a DVD in one or both eyes. The magnitude of DVD ranged from 1.5 to 5.5° (3$^{\Delta}$-10$^{\Delta}$). The size of the DVDs tended to increase in animals with larger esodeviations.

Figure 1C shows that each of the 7 strabismic monkeys also exhibited latent and/or manifest latent nystagmus. The velocity of the nystagmus slow phases ranged from a mean 0.5% to 1.7°/s. In monkeys fitted with binocular search coils, analysis of the waveforms verified that they conformed to the standard definition of latent/manifest latent nystagmus, ie, linear or decreasing-velocity profiles.[12] Figure 1D plots a nasal bias index ([nasalward eye

speed − temporalward]/[nasalward + temporalward] × 100) for smooth pursuit of horizontal target motion (approximately 1° spot) at 30°/s, and/or optokinetic nystagmus evoked by vertically oriented, high-contrast stripes (5° width) at 30°/s. An index of 0 = no bias and an index of 100 = 100% bias. Nasal bias indices ranged from 4 to 30 and tended to increase in concert with the severity of the other ocular motor signs.

Binocular Connections in Striate Cortex (Visual Area V1)

To determine if there was a relationship between the severity of the ocular motor signs and anatomic connections for binocularity, we analyzed horizontal axonal connections between ODCs in area V1 (striate cortex). Injections of the tracer BDA were made into individual ODCs in V1 of each cerebral hemisphere. BDA is taken up by individual neuron bodies and axonal terminals at the site of injection. Over a survival time of 7 to 10 days, the tracer is actively transported within neurons to anterogradely and retrogradely label connections to neurons in neighboring ODCs (anterograde = transport from pyramidal neuron body to axonal terminal connections; retrograde = transport from axonal terminal connections to pyramidal neuron body). Previous work in our laboratory has revealed a relationship between the overall pattern of BDA-labeling, viewed at low power in individual sections, and individual neuron counts obtained at higher power.[10,11] When the pattern appears as a "sunburst" distribution of label across ODCs (ie, an oval, densest at the injection center and diminishing uniformly in intensity of labeling with increasing distance from the center), counts tend to show comparable numbers of labeled neurons in right versus left eye ODCs. The "sunburst" pattern of labeling is therefore designated the "binocular connection" pattern. Alternatively, when the pattern appears as a "skipping" distribution of label across ODCs (also densest at the center but fluctuating in intensity of labeling across every other row of ODCs), counts tend to show higher numbers of labeled neurons in ODCs, which have the same ocularity as the injected ODC, and significantly lower numbers of labeled neurons in the ODCs of opposite ocularity. The "skipping" pattern of labeling is therefore designated the "monocular connection" pattern.

Figure 2 shows these dichotomous labeling patterns for six representative V1 injections: 3 of the "binocular/sunburst" variety in the normal monkeys (left column) and three of the "monocular/skipping" variety in the esotropic animals (right column, sections cut tangential to the pial surface after unfolding of the cortex; arrows indicate ODC rows of the same ocularity as the injected ODC). Each injection in V1 of both cerebral hemispheres was scored as binocular versus monocular for 6 of the 7 esotropic monkeys (Figure 3). The lowest proportion of monocular pattern (45%) was found in the normal monkeys and the highest proportion (up to 80%) in the esotropic animals (proportions test, $p = 0.04$).[13] The proportion of monocular pattern injections increased as a function of the magnitude of the ocular motor deficits (plotted for comparison in the regression line graph above), with some individual variation from animal to animal.

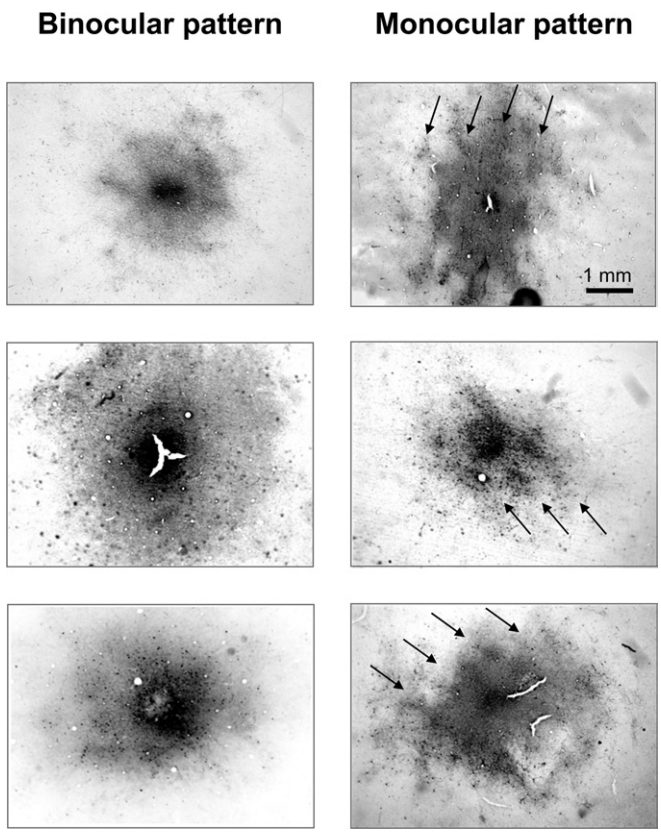

FIG 2. Biotinylated-dextran-amine (BDA) tracer injection sites in V1 layer 4B viewed at lower power. Three binocular "sunburst" patterns of labeling in the normal monkeys, and three monocular "skipping" patterns in the esotropic monkeys. Arrows in the monocular patterns indicate same-eye ocular dominance columns (every other row of ODCs) labeled more intensely at low power, corresponding to greater numbers of labeled neurons when viewed at higher power. Sections (40 μm thick) cut tangential to the pial surface.

Orbital and Extraocular Muscle Anatomy

A further goal of our study was to determine whether the ocular motor deficits in the strabismic monkeys could be attributed to abnormalities of the medial and/or lateral rectus muscles in each orbit. For this analysis, we carried out MRI and histologic studies of the 2 monkeys with the largest esotropias (monkeys T and H) and compared their horizontal rectus muscles to those in the normal animals. The orbits of each animal were first scanned using 1.5 Tesla MRI surface coils to measure pulley locations and muscle paths. Axial scans were obtained as well as serial, quasi-coronal images (1.5 mm thick planes), yielding resolutions of approximately 200 μm. The orbits were then embedded in paraffin and sectioned in coronal planes at 10 μm thickness before histologic staining. Digital, high-resolution images of the histologic sections were analyzed

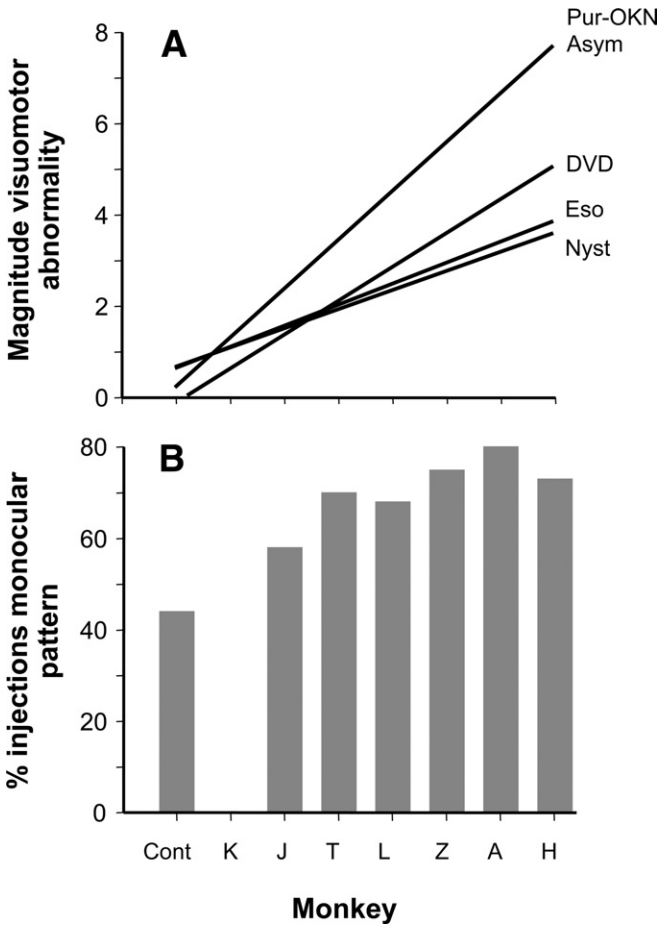

FIG 3. (A) Severity of ocular motor deficits. The regression lines plot the magnitude of the deficit in multiples normalized to the average value of the monkey with the mildest deficit (monkey K). (B) Proportion of V1 injections that corresponded to monocular patterns of neuronal labeling. Anatomic injections were not performed in monkey K. *Pur-OKN Asym*: pursuit or OKN nasal bias index; *DVD*: dissociated vertical deviation; *Eso*: esotropia; *Nyst*: latent nystagmus; *cont*: control.

quantitatively (for a more detailed description of these methods, see refs. 7-9).

The results of this analysis are summarized in Table 1. Cross-sectional areas of the rectus muscles, comparing medial to lateral rectus muscles in each group of monkeys, were comparable (the two esotropic monkeys were larger animals, with body weights and orbital volumes approximately twofold that of the controls). In both groups of monkeys, lateral rectus muscles had greater mean cross-sectional areas than medial rectus muscles. Orbital pulley inflections and muscle plane paths of the horizontal recti were also equivalent in esotropic versus normal monkeys (measured in serial planes, traveling from the orbital apex posteriorly to the muscle insertions anteriorly; the lateral rectus muscles conform to a more divergent nasal-to-temporal trajectory in the orbit). High-power imaging of individual muscle fibers and muscle elastin revealed no systematic differences. The medial rectus and lateral rectus muscles exhibited distinct global and orbital layers, with no distinction between esotropic and normal monkeys. Neuronal innervation densities were likewise indistinguishable in the two groups of monkeys, with higher densities for the lateral rectus muscles. Peak saccadic velocities are listed because these are known to be sensitive functional indicators for extraocular myopathy, abnormal contractility, and reduced lower motor neuron (oculomotor or abducens) innervation.[14] Abducting velocities exceeded adducting velocities in the normal and esotropic monkeys.

Discussion

The purpose of this study was to report findings in a series of primates who had onset of natural esotropia in the first months of life. The first question we posed was whether infantile esotropia in monkeys was an all-or-none disorder—do the animals exhibit equally severe deficits (eg, all large-angle strabismus and high-velocity nystagmus), or do they show a range of abnormality, from subtle to marked? The answer to this question is that they—like their human counterparts—display a range of quantitative severities. The esotropia in this group of animals spanned small to large and was constant, concomitant, and not related directly to refractive error. The majority of the animals freely alternated fixation; a minority displayed a consistent fixation preference. These features remarkably mimic features of early onset esotropia in human infants.[1,15]

Our findings also reveal systematic relationships among the classical ocular motor signs of infantile strabismus. Each of the esotropic animals displayed the constellation of signs that typify the infantile esotropia syndrome in humans: constant heterotropia, latent nystagmus, pursuit/OKN asymmetry, and—in five of six measured—DVD. The magnitude of each sign, with small individual variation, increased in concordance with the other signs. Similar concordance between these signs has been reported in normal infant primates exposed to binocular decorrelation in the first weeks of life.[2,3] In those monkeys, each sign increased in severity with increasing duration of the decorrelation. In a small group of adult humans who had infantile esotropia, a crude correlation was found between magnitude of esotropia, severity of pursuit asymmetry, velocity of latent nystagmus, and DVD.[16] We are unaware of other studies that have examined these interrelations. The relationship is deserving of more study because it has important implications for the mechanisms linking vergence and gaze dysfunction.

The second question we posed was whether the severity of the ocular motor signs was related to the severity of reduced binocular connections in area V1. Area V1 is the first locus in the primate central nervous system for binocularity, and binocularity provides the absolute disparity signals necessary to guide vergence alignment.[17,18] Binocular output from area V1 to regions of extrastriate cortex is also important for development of stable gaze holding

Table 1. Analysis of horizontal rectus muscle anatomy and function in normal and naturally esotropic monkeys

	Rectus muscle	Normal monkey	Naturally esotropic	*p*-value
Cross-sectional area (mm^2)	LR	13.6 ± 1.4	24.1 ± 7.9	NS, $p = 0.13$
	MR	11.5 ± 2.6	20.2 ± 7.6	NS, $p = 0.10$
Axial plane paths (slope $n - t$ / $p - a$)	LR	1.06 ± 0.03	1.05 ± 0.02	NS, $p = 0.98$
	MR	0.08 ± 0.01	0.07 ± 0.01	NS, $p = 0.74$
Innervation density (nerve area/EOM area)	LR	1.26	1.02	NS, $p = 0.56$
	MR	0.96	0.90	NS, $p = 0.90$
Peak saccadic velocity (10°, deg/s)	Ab	498 ± 54	532 ± 70	NS, $p = 0.70$
	Ad	472 ± 63	515 ± 44	NS, $p = 0.64$

LR: lateral rectus; *MR*: medial rectus; *NS*: not significant; *EOM*: extraocular muscle; *Ab*: abduction; *Ad*: adduction; *n-t*: nasal-temporal; *p-a*: posterior-anterior.

(absence of eye drift) and symmetric tracking.[19] Disruptions of normal binocular development in the first months of life lead to permanent deficits of these functions, manifested as nasalward drift (latent nystagmus) and nasalward biases of pursuit/OKN. Our finding that reduced anatomic connections for binocularity in the esotropic monkeys related systematically to their vergence and gaze deficits reinforces the validity of this functional-structural linkage.

The third question we addressed was whether early onset esotropia in primates could be explained by primary abnormalities of the horizontal rectus muscles. The answer is no; we found no evidence of a structural or innervational extraocular muscle anomaly. It may be useful in future experiments to also examine muscle composition using electron microscopy and immunohistochemistry. Our findings add to a large body of work in primate models, and to clinical observations, arguing against a primary extraocular muscle, motor neuron, or brainstem abnormality as the cause of infantile strabismus. We performed this analysis using a tedious method requiring serial sectioning of paraffin-embedded whole orbits, which has proven to be highly enlightening for revealing subtle abnormalities of orbital anatomy.[7-9]

Human infants at greatest risk of esotropia are those who suffer often subtle, direct or indirect perturbations to the geniculostriate pathways of the cerebral hemispheres during an early critical stage of visuomotor development.[20-22] Experiments in normal infant monkeys have revealed that sensorial, binocular decorrelation alone is sufficient to produce all of the ocular motor and sensory signs of this syndrome, without any manipulation of the EOMs or motor pathways.[2,3] Taken together, the current results and those of previous animal and human studies lead us to conclude that infantile esotropia is a natural default. The default is brought about when immature, unstable, nasally biased vergence and gaze circuits are impeded in their normal maturation, by intrinsic or extrinsic factors, during the first critical weeks and months of life.

References

1. Fu VLN, Stager DR, Birch EE, Progression of intermittent, small angle, and variable infantile esotropia. Invest Ophthalmol Vis Sci 2007; 48:661-4.
2. Wong AMF, Foeller P, Bradley D, Burkhalter A, Tychsen L. Early versus delayed repair of infantile strabismus in macaque monkeys: I. Ocular motor effects. J AAPOS 2003;7:200-9.
3. Tychsen L, Wong AMF, Foeller P, Bradley D. Early versus delayed repair of infantile strabismus in macaque monkeys: II. Effects on motion visually evoked responses. Invest Ophthalmol Vis Sci 2004; 45:821-7.
4. Quick MW, Boothe RG. A photographic technique for measuring horizontal and vertical eye alignment throughout the field of gaze. Invest Ophthalmol Vis Sci 1992;33:234-46.
5. Foeller P, Tychsen L. Eye movement training and recording in alert macaque monkeys: 1. Operant visual conditioning. 2. Magnetic search coil and head restraint surgical implantation. 3. Calibration and recording. Strabismus 2002;10:5-22.
6. Scott C, Gusdorf G, Tychsen L. Automated cover test for eye misalignment in awake monkeys using spectacle-mounted liquid crystal shutters. Binocul Vis Strabismus Q 1999;15:59-66.
7. Demer JL. Pivotal role of orbital connective tissues in binocular alignment and strabismus. Invest Ophthalmol Vis Sci 2004;45:729-38.
8. Demer JL, Poukens V, Miller JM, Micevych P. Innervation of extraocular pulley smooth muscle in monkeys and humans. Invest Ophthalmol Vis Sci 1997;38:1774-85.
9. Narasimhan A, Tychsen L, Poukens V, Demer JL. Horizontal rectus muscle anatomy in naturally and artificially strabismic monkeys. Invest Ophthalmol Vis Sci 2007;48:2576-88.
10. Tychsen L, Burkhalter A. Neuroanatomic abnormalities of primary visual cortex in macaque monkeys with infantile esotropia: Preliminary results. J Pediatr Ophthalmol Strabismus 1995;32:323-8.
11. Tychsen L, Wong AMF, Burkhalter A. Paucity of horizontal connections for binocular vision in V1 of naturally-strabismic macaques: Cytochrome-oxidase compartment specificity. J Comp Neurol 2004; 474:261-75.
12. N.E.I./N.I.H. Committee. A classification of eye movement abnormalities and strabismus (CEMAS). Report of a National Eye Institute sponsored workshop. Bethesda (MD): National Eye Institute, National Institute of Health; February 2001;9-10.
13. Walsh JE. Handbook of Nonparametric Statistics. Princeton (NJ): Van Nostrand Company; 1968.
14. Leigh RJ, Zee DS. The Neurology of Eye Movements. 3rd ed. New York: Oxford University Press; 1999.
15. Tychsen L. Infantile esotropia: Current neurophysiologic concepts. In: Rosenbaum AL, Santiago AP, editors. Clinical strabismus management. Philadephia (PA): WB Saunders; 1999. p. 117-38.
16. Tychsen L, Lisberger SG. Maldevelopment of visual motion processing in humans who had strabismus with onset in infancy. J Neurosci 1986;6:2495-508.
17. Masson GS, Busettini C, Miles FA. Vergence eye movements in response to binocular disparity without depth perception. Nature 1997;389:283-6.
18. Cumming BG, Parker AJ. Responses of primary visual cortical neurons to binocular disparity without depth perception. Nature 1997; 389:280-3.
19. Tychsen L. Strabismus: The scientific basis. In: Taylor D, Hoyt CS, editors. Pediatric ophthalmology and strabismus. 3rd ed. Edinburgh: Elsevier Saunders; 2005. p. 836-48.
20. van Hof-van Duin J, Evenhuis-van Leunen A, Mohn G, Baerts W, Fetter WPF. Effects of very low birth weight (VLBW) on visual

development during the first year after term. Early Hum Dev 1989;20:255-66.
21. Pike MG, Holmstrom G, de Vries LS, Pennock JM, Drew KJ, Sonksen PM, Dubowitz LM, et al. Patterns of visual impairment associated with lesions of the preterm infant brain. Dev Med Child Neurol 1994;36:849-62.
22. Jacobson LK, Dutton GN. Periventricular leukomalacia: An important cause of visual and ocular motility dysfunction in children. Surv Ophthalmol 2002;45:1-13.
23. Tychsen L. Causing and curing infantile esotropia in primates: The role of decorrelated binocular input. Tr Am Ophth Soc 2007;105:564-93.

First Person

Panda ERG

Eleven-year-old Andrea couldn't see very well—she was sensitive to light, and she had no sight in the dark. Dr. H., Andrea's ophthalmologist, knew that her retina was not working properly. Andrea had already been through several ERG tests, and like any child, Andrea didn't like ERGs, she didn't like contact lens electrodes, and she didn't like to sit in the dark with her eyes patched. Andrea was brave, but she had never allowed both eyes to be tested at the same time.

Dr. H. said that it was time for another test. Andrea started to cry as soon as the eye drops were administered. Rita, the ERG assistant, pulled a large white-and-black panda bear with big eyes out of a basket of toys. These toys were meant for children who had completed their testing, but Rita offered it to Andrea beforehand. Andrea snuggled with the Panda, and didn't notice the time pass as she sat in the dark with both eyes patched. I asked Rita to try to test both eyes at once, and when the contact lens electrodes were placed in each eye, Andrea clutched her new panda tightly in her arms but didn't stop crying. This caused the ERG recording to give only artifacts, with no true responses from the girl's eyes.

Rita started to tell a story, a story about Andrea and the panda. Andrea and the panda went to the park, where they were playing and eating ice cream. The panda was a messy eater, and he had to wash his sticky paws in the fountain. He cleaned his fingers but then fell in and was soaked. So Andrea and the panda went home, where she found a hair drier and blow dried her friend's fur. The panda didn't like that, and by the time he was finally dry, they were hungry again. Of course, the panda wasn't good with the food and had to wash his paws again . . .

Andrea stopped crying, opened her eyes, and listened to the story. Rita was able to record excellent waveforms. When Rita opened the door, she continued the story about the panda and Andrea and their day. It was silent outside the testing room, where everyone had been listening to the story.

—Christina Gerth, MD